Acta Cryst. (1978). B**34**, 2699–2707

The Crystal Structures of Nine K Feldspars from the Adamello Massif (Northern Italy)

By A. Dal Negro, R. De Pieri and S. Quareni

Istituto di Mineralogia e Petrologia, Università di Padova, Italy

and W. H. Taylor

Cavendish Laboratory, Cambridge, England

(*Received* 14 *February* 1978; *accepted* 2 *May* 1978)

The crystal structures of nine K feldspars from the Adamello Massif have been refined. Three of the specimens show (geometrical) monoclinic symmetry, and six cover the range between 'monoclinic' and maximum triclinicity. Of the three 'monoclinic' samples one is also structurally monoclinic to within the accuracy achieved, but two must be considered truly triclinic on the basis of the structural detail. A discussion of Al ordering in the $T_1(0)$ site in the structure leads to the conclusion that the ordering process in the Adamello materials is intermediate between the one-step and the two-step types. Since these K feldspars are certainly untwinned, it is concluded that they have crystallized (or recrystallized) directly with triclinic symmetry, and have not inverted from a primary monoclinic disordered phase through an ordering due to a diffusive process.

1. Introduction

Recently De Pieri & Callegari (1977), while studying the potassium feldspars in rocks from the Adamello Massif in Northern Italy, found untwinned homogeneous crystals having different degrees of triclinicity over the whole range from orthoclase to maximum microcline. Information obtained from the refinement of the crystal structures of nine of these materials supplements that already published about several 'monoclinic' varieties of K feldspar, two maximum microclines and one intermediate microcline (see, for example, Smith, 1974). The results obtained are applied to the discussion of the relationship between triclinicity and the (Al,Si) ordering in the structure, and provide the basis of an attempt to elucidate the nature of the ordering process.

Experimental details are given in § 2, the procedure used in structural refinement is outlined in § 3, and the results obtained are set out in Tables 1 to 9. § 4 treats in more detail the complexities of the final stages of the refinement process in relation to the (Al,Si) occupancies

Table 1. *Chemical composition* (*from Callegari, De Pieri, Mezzacasa & Piccirillo,* 1974) *and cell parameters*

	P2B	P2A	CA1A	P17C	A1D	CA1B	P1C	RC20C	CA1E
K_2O	16.02	16.02	15.18	14.98	15.34	15.18	15.24	14.52	15.18
Na_2O	0.63	0.63	1.12	1.35	0.95	1.12	0.98	1.49	1.12
CaO	0.18	0.18	0.06	0.02	0.10	0.06	0.10	0.18	0.06
BaO	0.26	0.26	0.68	0.02	0.36	0.68	0.37	0.18	0.68
Rb_2O	–	–	–	0.26	–	–	–	–	–
Or	93.1	93.1	88.6	87.1	90.4	88.6	90.0	85.5	88.6
Ab	5.5	5.5	9.9	12.0	8.5	9.9	8.8	13.3	9.9
An	0.9	0.9	0.3	0.1	0.5	0.3	0.5	0.9	0.3
Cn	0.5	0.5	1.2	0.0	0.6	1.2	0.7	0.3	1.2
$Rb_{feld.}$	–	–	–	0.8	–	–	–	–	–
a	8.589(2)Å	8.583(2)Å	8.563(2)Å	8.567(2)Å	8.564(2)Å	8.560(2)Å	8.574(2)Å	8.567(2)Å	8.561(2)Å
b	13.013(7)	12.988(7)	12.990(7)	12.980(7)	12.984(7)	12.984(7)	12.962(7)	12.970(7)	12.972(7)
c	7.197(2)	7.202(2)	7.210(2)	7.200(2)	7.201(2)	7.209(2)	7.210(2)	7.221(2)	7.223(2)
α	90°	90°	90°	90°11'	90°18'	90°37'	90°48'	91°0'	91°25'
β	116°1'	116°3'	115°56'	116°2'	116°1'	116°2'	116°2'	116°0'	115°58'
γ	90°	90°	90°	89°42'	89°28'	88°53'	88°36'	88°14'	87°33'
α^*	90°	90°	90°	90°3'	90°5'	90°9'	90°12'	90°15'	90°23'
γ^*	90°	90°	90°	90°15'	90°27'	90°56'	91°10'	91°28'	92°2'
V	722.9Å^3	721.3Å^3	721.2Å^3	719.5Å^3	719.5Å^3	719.8Å^3	719.7Å^3	720.7Å^3	720.5Å^3
F_{000}	550.96	550.96	550.56	548.74	550.14	550.56	550.19	548.58	550.56
Total number of reflections	2088	2088	2047	2093	2079	2095	2091	2092	2097
Reflections with $I>2\sigma(I)$	1638	1587	1640	1738	1907	1637	1455	1773	1737
R_{final}	3.4	3.4	3.6	3.2	2.4	3.8	5.3	3.5	2.8

of the tetrahedral sites, and in § 5 there is a discussion of the structural symmetry of 'monoclinic' potassium feldspars. The nature of the ordering process in these and other feldspars is considered in § 6.

The relation between cell parameters, optical characteristics and (Al,Si) ordering for the Adamello feldspars will be discussed in a forthcoming paper.

2. Experimental details

The crystals used came from tonalites, quartz diorites, aplite and pegmatite dykes of the Adamello Massif. Their compositions are shown in Table 1 as percentages of alkali and alkaline-earth elements and also as molar percentages of the feldspar end-members Or, Ab, An, Cn and Rb feldspar.

The cell parameters, also listed in Table 1, were derived from diffractometer measurements at high angles with Mo $K\alpha$ radiation. Values of α^* and γ^* are plotted in Fig. 1. It should be noted that in this group of materials it is not unusual for crystals with different degrees of triclinicity to occur in the same rock sample: thus, in Table 1, rock sample CA1 with crystals CA1A, CA1B, CA1E and rock sample P2 with crystals P2A and P2B.

Intensity data were collected for each crystal on a Philips PW 1100 four-circle diffractometer; Mo $K\alpha$ radiation, monochromatized with a graphite crystal,

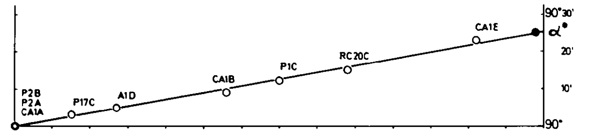

Fig. 1. $\alpha^* - \gamma^*$ plot of the Adamello K feldspars. The solid circle is the $\alpha^* - \gamma^*$ plot of maximum microcline (Smith, 1974, p. 258).

Table 2. *Atomic coordinates*

Estimated standard errors are in parentheses and refer to the last decimal place.

	P2B			P2A			CA1A		
	x	y	z	x	y	z	x	y	z
K/Na	0.2850(1)	0.9998(1)	0.1378(1)	0.2851(1)	0.9996(1)	0.1380(1)	0.2840(1)	0.9993(1)	0.1375(1)
$T_1(0)$	.0097(1)	.1850(1)	.2237(1)	.0095(1)	.1852(1)	.2236(1)	.0096(1)	.1846(1)	.2235(1)
$T_1(m)$	.0095(1)	.8151(1)	.2241(1)	.0096(1)	.8152(1)	.2247(1)	.0095(1)	.8160(1)	.2252(1)
$T_2(0)$	.7093(1)	.1179(1)	.3442(1)	.7096(1)	.1181(1)	.3442(1)	.7087(1)	.1180(1)	.3441(1)
$T_2(m)$	.7092(1)	.8822(1)	.3446(1)	.7093(1)	.8823(1)	.3447(1)	.7082(1)	.8826(1)	.3451(1)
$O_A(1)$	.9997(3)	.1459(2)	.9998(3)	.9996(3)	.1458(2)	.9983(3)	.9999(3)	.1452(2)	.9981(3)
$O_A(2)$	.6373(3)	.0002(2)	.2852(3)	.6382(3)	.0003(2)	.2854(3)	.6355(3)	.0006(2)	.2855(3)
$O_B(0)$	.8275(3)	.1471(2)	.2270(3)	.8267(3)	.1469(2)	.2270(3)	.8261(3)	.1457(2)	.2271(4)
$O_B(m)$	.8277(3)	.8534(2)	.2275(4)	.8276(3)	.8533(2)	.2276(3)	.8268(3)	.8544(2)	.2290(4)
$O_C(0)$	.0357(3)	.3115(2)	.2582(3)	.0357(3)	.3119(2)	.2579(3)	.0353(3)	.3123(2)	.2582(3)
$O_C(m)$	.0352(3)	.6892(2)	.2590(3)	.0354(3)	.6888(2)	.2597(3)	.0353(3)	.6893(2)	.2601(3)
$O_D(0)$	.1812(3)	.1260(2)	.4054(3)	.1810(3)	.1260(2)	.4062(3)	.1826(3)	.1255(2)	.4065(3)
$O_D(m)$	.1804(3)	.8738(2)	.4057(3)	.1801(3)	.8738(2)	.4066(3)	.1809(3)	.8742(2)	.4074(3)

	P17C			A1D			CA1B		
	x	y	z	x	y	z	x	y	z
K/Na	0.28447(8)	0.99911(6)	0.1379(1)	0.28420(6)	0.99866(4)	0.13764(8)	0.2837(1)	0.9967(1)	0.1375(1)
$T_1(0)$	.00955(9)	.18492(5)	.2234(1)	.00951(7)	.18514(4)	.22282(8)	.0099(1)	.1858(1)	.2214(1)
$T_1(m)$	.00949(9)	.81582(5)	.2251(1)	.00938(6)	.81611(4)	.22545(8)	.0094(1)	.8173(1)	.2277(1)
$T_2(0)$	.70929(8)	.11813(5)	.3440(1)	.70914(6)	.11820(4)	.34362(7)	.7094(1)	.1189(1)	.3425(1)
$T_2(m)$	.70851(8)	.88251(5)	.3449(1)	.70810(6)	.88282(4)	.34530(7)	.7070(1)	.8836(1)	.3470(1)
$O_A(1)$	.0004(2)	.1455(1)	.9979(3)	.0004(2)	.1454(1)	.9969(2)	.0003(3)	.1448(2)	.9926(4)
$O_A(2)$	.6372(2)	.0005(1)	.2853(3)	.6363(2)	.0010(1)	.2851(2)	.6356(3)	.0024(2)	.2853(3)
$O_B(0)$	.8263(2)	.1465(2)	.2266(3)	.8258(2)	.1463(1)	.2261(2)	.8239(3)	.1465(2)	.2238(4)
$O_B(m)$	.8276(2)	.8541(2)	.2293(3)	.8276(2)	.8546(1)	.2299(2)	.8281(3)	.8555(2)	.2329(4)
$O_C(0)$	.0353(2)	.3122(1)	.2582(3)	.0351(2)	.3126(1)	.2574(2)	.0345(3)	.3150(2)	.2562(3)
$O_C(m)$	.0357(2)	.6893(1)	.2604(3)	.0353(2)	.6901(1)	.2605(2)	.0358(3)	.6916(2)	.2636(4)
$O_D(0)$	.1824(2)	.1257(1)	.4067(3)	.1827(2)	.1255(1)	.4067(2)	.1857(3)	.1248(2)	.4062(3)
$O_D(m)$	.1800(2)	.8741(1)	.4070(3)	.1799(2)	.8741(1)	.4074(2)	.1794(3)	.8741(2)	.4090(3)

	P1C			RC20C			CA1E		
	x	y	z	x	y	z	x	y	z
K/Na	0.2837(2)	0.9960(1)	0.1372(2)	0.2830(1)	0.9950(1)	0.1372(1)	0.28232(7)	0.99328(5)	0.13640(9)
$T_1(0)$	.0097(2)	.1865(1)	.2205(2)	.0098(1)	.1865(1)	.2193(1)	.01002(8)	.18710(5)	.21754(9)
$T_1(m)$	.0094(2)	.8176(1)	.2286(2)	.0095(1)	.8184(1)	.2298(1)	.00959(8)	.81950(4)	.23165(9)
$T_2(0)$	.7105(2)	.1192(1)	.3421(2)	.7101(1)	.1195(1)	.3415(1)	.71020(7)	.11998(4)	.34043(9)
$T_2(m)$	.7073(2)	.8840(1)	.3480(2)	.7065(1)	.8845(1)	.3484(1)	.70518(7)	.88532(4)	.35005(9)
$O_A(1)$	.0007(4)	.1451(3)	.9901(5)	.0000(3)	.1444(2)	.9875(3)	.0004(2)	.1445(1)	.9839(2)
$O_A(2)$	.6368(4)	.0039(2)	.2849(5)	.6356(3)	.0037(2)	.2856(3)	.6345(2)	.0050(1)	.2862(2)
$O_B(0)$	.8237(4)	.1480(3)	.2224(5)	.8223(3)	.1469(2)	.2225(3)	.8209(2)	.1467(1)	.2202(3)
$O_B(m)$	.8290(4)	.8562(3)	.2348(5)	.8296(3)	.8562(2)	.2362(3)	.8308(2)	.8575(1)	.2396(3)
$O_C(0)$	.0353(4)	.3163(2)	.2549(5)	.0349(3)	.3173(2)	.2544(3)	.0341(2)	.3188(1)	.2523(3)
$O_C(m)$	.0371(4)	.6930(3)	.2646(5)	.0372(3)	.6934(2)	.2667(3)	.0371(2)	.6953(1)	.2690(3)
$O_D(0)$	.1860(4)	.1248(3)	.4053(5)	.1875(3)	.1238(2)	.4059(3)	.1900(2)	.1234(1)	.4050(2)
$O_D(m)$	.1768(4)	.8740(3)	.4084(5)	.1775(3)	.8741(2)	.4108(3)	.1763(2)	.8745(1)	.4113(2)

was used to measure reflections up to $2\theta = 60°$ by the ω-scan method with 5 s background counts on either side of the peak. No absorption corrections were required for the very small crystals used. From these measurements values of F_{obs} and σF_{obs} were derived by the method of Davies & Gatehouse (1973).

3. Refinement of structures

The full-matrix least-squares program *ORFLS* (Busing, Martin & Levy, 1962) was used for refinement of the structures. Only those structure amplitudes were included for which F_{obs} was greater than twice the standard deviation in F_{obs} as determined by counting statistics: for each crystal the total number of observed reflections and the number included in the structure refinement are shown in Table 1.

Atomic scattering factors were taken from *International Tables for X-ray Crystallography* (1962). For the large cation (K,Na,Ca,Ba,Rb) the effective scattering factor was calculated for each crystal from the chemical analysis. For the tetrahedral atoms a common weighted scattering factor $(0{\cdot}25f_{\text{Al}} + 0{\cdot}75f_{\text{Si}})$ was assumed for the first stage of refinement, but this was modified for each of the four tetrahedral sites as the actual (Al,Si) occupancies gradually emerged in the course of the refinement; the final stage in the complex refinement procedure is discussed more fully in § 4.

Table 1 shows that crystals P2B, P2A and CA1A are geometrically monoclinic, with $\alpha = \gamma = 90°$ within experimental error (which is estimated as $\sim 2'$). Goldsmith & Laves (1954) have shown that in orthoclases and adularias a 'monoclinic' pattern may result from the existence of a balanced twin domain structure of triclinic units on a sufficiently fine scale. In a detailed discussion of these three crystals (§ 5) the true symmetry of the samples P2A and CA1A is found to be $C\bar{1}$ as for the geometrically triclinic materials, but, to a high degree of accuracy, $C2/m$ in agreement with the geometrical symmetry for the sample P2B.

The results of the refinements of the structures are given in Tables 2–5, and the residuals (*R* final) in Table 1.†

Table 3 lists the T—O tetrahedral distances of the nine samples studied; as in Table 1 the geometrically triclinic samples are listed in order of increasing α^* and γ^*, while the first three (geometrically monoclinic) samples are listed in order of increasing structural triclinicity. It is interesting to note that samples CA1A and P17C, the first geometrically monoclinic, the second geometrically slightly triclinic, show an inverted order of structural triclinicity: for instance, T_1—O average distances are greater in CA1A than in P17C.

The K—O distances (Table 4) show that with increasing amounts of Al in $T_1(0)$ sites, *i.e.* with increasing (Al,Si) order, the K atom moves slightly away from $O_B(m)$, $O_C(m)$ and $O_D(m)$, but towards $O_B(0)$, $O_C(0)$ and $O_D(0)$. The influence of the triclinicity on these K—O bond distances is shown in Fig. 2 where the difference $\Delta O = [K{-}O_j(m)] - [K{-}O_j(0)]$ is plotted against the $T_1(0)$ mean distance for each sample. From this diagram it is clear that the

---

† Lists of structure factors and anisotropic thermal parameters for the nine compounds have been deposited with the British Library Lending Division as Supplementary Publication No. SUP 33593 (129 pp.). Copies may be obtained through The Executive Secretary, International Union of Crystallography, 5 Abbey Square, Chester CH1 2HU, England.

Table 3. *Tetrahedral bond lengths* (Å)

Estimated standard errors are in parentheses and refer to the last decimal place.

	P2B	P2A	CA1A	P17C	A1D	CA1B	P1C	RC20C	CA1E
$T_1(0)-O_A(1)$	1.656(2)	1.667(2)	1.671(2)	1.671(2)	1.673(2)	1.695(2)	1.708(3)	1.719(2)	1.731(2)
$-O_B(0)$	1.651(2)	1.657(2)	1.662(2)	1.659(2)	1.667(2)	1.688(2)	1.689(4)	1.711(2)	1.731(2)
$-O_C(0)$	1.664(2)	1.665(2)	1.678(2)	1.672(2)	1.675(1)	1.696(2)	1.703(3)	1.718(2)	1.728(2)
$-O_D(0)$	1.667(2)	1.671(2)	1.678(2)	1.674(2)	1.679(1)	1.698(2)	1.703(4)	1.720(2)	1.735(2)
Mean	1.660	1.665	1.672	1.669	1.674	1.694	1.701	1.717	1.731
$T_1(m)-O_A(1)$	1.658(2)	1.653(2)	1.655(2)	1.649(2)	1.647(2)	1.635(2)	1.621(4)	1.616(2)	1.602(2)
$-O_B(m)$	1.649(2)	1.648(2)	1.653(2)	1.646(2)	1.643(2)	1.636(2)	1.633(4)	1.623(2)	1.613(2)
$-O_C(m)$	1.658(2)	1.661(2)	1.664(2)	1.661(2)	1.655(1)	1.651(2)	1.635(4)	1.641(2)	1.630(2)
$-O_D(m)$	1.663(2)	1.660(2)	1.663(2)	1.659(2)	1.658(1)	1.649(2)	1.633(3)	1.638(2)	1.627(2)
Mean	1.657	1.655	1.659	1.654	1.651	1.643	1.631	1.630	1.618
$T_2(0)-O_A(2)$	1.636(2)	1.634(2)	1.632(2)	1.634(2)	1.633(1)	1.628(2)	1.613(3)	1.623(2)	1.621(2)
$-O_B(0)$	1.624(2)	1.615(2)	1.611(2)	1.614(2)	1.612(2)	1.606(2)	1.609(4)	1.595(2)	1.592(2)
$-O_C(m)$	1.634(2)	1.629(2)	1.626(2)	1.622(2)	1.626(2)	1.624(2)	1.629(4)	1.624(2)	1.628(2)
$-O_D(m)$	1.629(2)	1.624(2)	1.622(2)	1.622(2)	1.623(1)	1.620(2)	1.628(3)	1.619(2)	1.624(2)
Mean	1.631	1.626	1.623	1.623	1.624	1.620	1.620	1.615	1.616
$T_2(m)-O_A(2)$	1.641(2)	1.637(2)	1.639(2)	1.633(2)	1.635(1)	1.640(2)	1.649(3)	1.640(2)	1.644(2)
$-O_B(m)$	1.624(2)	1.623(2)	1.616(2)	1.617(2)	1.615(2)	1.616(2)	1.614(4)	1.618(2)	1.621(2)
$-O_C(0)$	1.626(2)	1.622(2)	1.614(2)	1.620(2)	1.620(2)	1.611(2)	1.605(3)	1.601(2)	1.600(2)
$-O_D(0)$	1.628(2)	1.623(2)	1.621(2)	1.617(2)	1.615(1)	1.608(2)	1.608(4)	1.603(2)	1.600(2)
Mean	1.630	1.626	1.623	1.622	1.621	1.619	1.619	1.615	1.616

pair of O_C atoms is the most sensitive to the variation of Al content in $T_1(0)$, and that the pair O_D is the least sensitive. The O_A atoms are only very slightly sensitive to the amount of Al in $T_1(0)$ (Table 4).

The mean values of the O–T–O bond angles (Table 5) are very similar for all the tetrahedra of the nine specimens studied. The distortions of individual tetrahedra, evaluated using the expression $\sigma = \sqrt{\{\sum_6 [(\mathrm{O{-}T{-}O}) - 109{\cdot}5°]^2/5\}}$ of Ribbe, Phillips & Gibbs (1972), are set out in Table 6. In a given feldspar $T_1(0)$ is more distorted than the other tetrahedra $T_1(m)$, $T_2(0)$ and $T_2(m)$, except in the case of specimen CA1E and perhaps in specimen P2A. There is a marked tendency for greater distortion in the highly-ordered feldspars except for the tetrahedra $T_1(m)$ in which the distortion is very similar in all nine materials. The calculations of distortion thus support the suggestion that it is due mainly to the (Al,Si) ordering in these K feldspars.

The mean values of the T–O–T bond angles (Table 5) are also very similar for the nine Adamello specimens, individual values varying from about 130 to 155° as has been found in previous feldspar studies. The effect of variation in (Al,Si) order on T–O–T

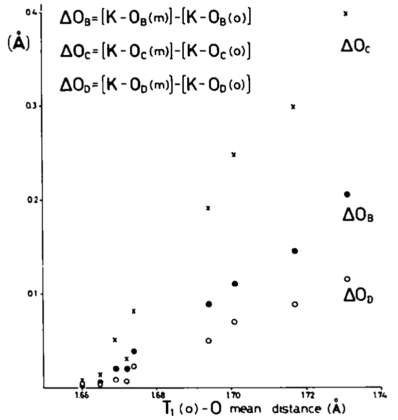

Fig. 2. Differences between pairs of K–O distances referring to oxygen pairs split by the loss of 2/*m* symmetry *vs* the triclinicity estimated from $T_1(0)$–O mean distances.

Table 4. *Interatomic distances* (Å)

Estimated standard errors are in parentheses and refer to the last decimal place.

	P2B	P2A	CA1A	P17C	A1D	CA1B	P1C	RC20C	CA1E
K/Na–$O_A(1)$	2.910(2)	2.909(2)	2.883(2)	2.891(2)	2.887(2)	2.881(2)	2.884(4)	2.873(2)	2.873(2)
–$O_A(1)$	2.904(2)	2.899(2)	2.895(2)	2.895(2)	2.894(2)	2.883(2)	2.888(4)	2.878(2)	2.875(2)
–$O_A(2)$	2.733(2)	2.738(2)	2.718(2)	2.728(2)	2.722(2)	2.721(2)	2.737(3)	2.732(2)	2.731(2)
–$O_A(2)$	3.391(3)	3.390(2)	3.408(2)	3.396(2)	3.399(2)	3.408(2)	3.398(4)	3.417(2)	3.425(2)
–$O_B(0)$	3.043(2)	3.040(2)	3.030(3)	3.030(2)	3.018(2)	2.991(3)	2.984(4)	2.971(2)	2.936(2)
–$O_B(m)$	3.044(2)	3.047(2)	3.050(3)	3.051(2)	3.057(2)	3.087(3)	3.095(4)	3.116(2)	3.141(2)
–$O_C(0)$	3.124(2)	3.113(2)	3.106(3)	3.094(2)	3.080(2)	3.023(3)	2.999(4)	2.974(2)	2.928(2)
–$O_C(m)$	3.132(3)	3.127(2)	3.137(3)	3.145(2)	3.162(2)	3.215(3)	3.247(4)	3.273(2)	3.327(2)
–$O_D(0)$	2.951(2)	2.956(2)	2.945(2)	2.946(2)	2.939(2)	2.919(2)	2.913(4)	2.901(2)	2.882(2)
–$O_D(m)$	2.955(2)	2.959(2)	2.952(2)	2.955(2)	2.962(2)	2.969(2)	2.983(4)	2.990(2)	2.998(2)
O–O distances									
in $T_1(0)$ O_A–O_B	2.643(3)	2.657(3)	2.663(3)	2.663(3)	2.669(2)	2.695(3)	2.709(5)	2.731(3)	2.750(2)
O_A–O_C	2.774(3)	2.782(3)	2.797(3)	2.792(3)	2.792(2)	2.832(3)	2.841(5)	2.867(3)	2.881(2)
O_A–O_D	2.651(3)	2.666(3)	2.674(3)	2.671(3)	2.678(2)	2.706(3)	2.717(5)	2.743(3)	2.764(2)
O_B–O_C	2.733(3)	2.741(3)	2.755(3)	2.750(3)	2.764(2)	2.804(3)	2.814(5)	2.850(3)	2.884(2)
O_B–O_D	2.745(3)	2.748(3)	2.758(3)	2.754(3)	2.758(2)	2.792(3)	2.801(5)	2.821(3)	2.847(2)
O_C–O_D	2.711(3)	2.714(3)	2.728(3)	2.719(3)	2.726(2)	2.765(3)	2.774(5)	2.801(3)	2.825(2)
Mean	2.709	2.718	2.729	2.725	2.731	2.766	2.776	2.802	2.825
in $T_1(m)$ O_A–O_B	2.645(3)	2.639(3)	2.647(3)	2.638(3)	2.636(2)	2.626(3)	2.615(5)	2.609(3)	2.595(2)
O_A–O_C	2.770(3)	2.769(3)	2.773(3)	2.765(3)	2.761(2)	2.753(3)	2.727(5)	2.734(3)	2.717(2)
O_A–O_D	2.649(3)	2.646(3)	2.655(3)	2.646(3)	2.642(2)	2.627(3)	2.606(5)	2.609(3)	2.591(2)
O_B–O_C	2.728(3)	2.727(3)	2.735(3)	2.724(3)	2.713(2)	2.694(3)	2.682(5)	2.667(3)	2.640(2)
O_B–O_D	2.736(3)	2.733(3)	2.739(3)	2.727(3)	2.725(2)	2.717(3)	2.695(5)	2.695(3)	2.677(2)
O_C–O_D	2.700(3)	2.699(3)	2.690(3)	2.685(3)	2.689(2)	2.675(3)	2.645(5)	2.648(3)	2.631(2)
Mean	2.705	2.702	2.707	2.698	2.694	2.682	2.662	2.660	2.642
in $T_2(0)$ O_A–O_B	2.665(3)	2.650(3)	2.645(3)	2.650(3)	2.656(2)	2.657(3)	2.658(5)	2.657(3)	2.667(2)
O_A–O_C	2.589(3)	2.582(3)	2.578(3)	2.577(3)	2.576(2)	2.568(3)	2.561(5)	2.562(3)	2.560(2)
O_A–O_D	2.652(3)	2.644(3)	2.641(3)	2.642(3)	2.639(2)	2.625(3)	2.621(5)	2.614(3)	2.604(2)
O_B–O_C	2.676(3)	2.669(3)	2.664(3)	2.662(3)	2.661(2)	2.659(3)	2.655(5)	2.649(3)	2.652(2)
O_B–O_D	2.688(3)	2.678(3)	2.674(3)	2.676(3)	2.676(2)	2.676(3)	2.683(5)	2.666(3)	2.673(2)
O_C–O_D	2.700(3)	2.693(3)	2.700(3)	2.696(3)	2.691(2)	2.675(3)	2.684(5)	2.667(3)	2.670(2)
Mean	2.662	2.653	2.650	2.651	2.650	2.643	2.644	2.636	2.638
in $T_2(m)$ O_A–O_B	2.663(3)	2.658(3)	2.653(3)	2.643(3)	2.637(2)	2.627(3)	2.619(5)	2.618(3)	2.605(2)
O_A–O_C	2.585(3)	2.579(3)	2.571(3)	2.577(3)	2.580(2)	2.575(3)	2.577(5)	2.565(3)	2.569(2)
O_A–O_D	2.654(3)	2.648(3)	2.648(3)	2.639(3)	2.645(2)	2.648(3)	2.661(5)	2.647(3)	2.655(2)
O_B–O_C	2.669(3)	2.665(3)	2.652(3)	2.662(3)	2.660(2)	2.654(3)	2.649(5)	2.649(3)	2.650(2)
O_B–O_D	2.690(3)	2.683(3)	2.677(3)	2.673(3)	2.668(2)	2.665(3)	2.661(5)	2.660(3)	2.654(2)
O_C–O_D	2.697(3)	2.694(3)	2.687(3)	2.686(3)	2.688(2)	2.681(3)	2.682(5)	2.680(3)	2.684(2)
Mean	2.660	2.654	2.648	2.647	2.646	2.642	2.642	2.636	2.636

Table 5. *Interatomic angles* (°)

Estimated standard errors are in parentheses and refer to the last decimal place.

	P2B	P2A	CA1A	P17C	A1D	CA1B	P1C	RC20C	CA1E
in $T_1(0)$									
O_A-T-O_B	106.1(1)	106.1(1)	106.1(1)	106.2(1)	106.09(8)	105.6(1)	105.8(2)	105.5(1)	105.22(9)
O_A-T-O_C	113.3(1)	113.2(1)	113.3(1)	113.2(1)	113.07(8)	113.2(1)	112.8(2)	113.1(1)	112.79(9)
O_A-T-O_D	105.8(1)	106.0(1)	106.0(1)	106.0(1)	106.07(7)	105.8(1)	105.6(2)	105.8(1)	105.80(9)
O_B-T-O_C	111.0(1)	111.2(1)	111.2(1)	111.3(1)	111.65(8)	111.9(1)	112.1(2)	112.4(1)	112.96(9)
O_B-T-O_D	111.6(1)	111.3(1)	111.4(1)	111.4(1)	111.06(8)	111.1(1)	111.3(2)	110.6(1)	110.45(9)
O_C-T-O_D	108.9(1)	108.9(1)	108.8(1)	108.7(1)	108.77(7)	109.1(1)	109.1(2)	109.2(1)	109.34(9)
Mean	109.5	109.5	109.5	109.5	109.45	109.5	109.5	109.4	109.43
in $T_1(m)$									
O_A-T-O_B	106.2(1)	106.2(1)	106.3(1)	106.4(1)	106.46(8)	106.8(1)	107.0(2)	107.3(1)	107.65(9)
O_A-T-O_C	113.3(1)	113.4(1)	113.3(1)	113.3(1)	113.53(8)	113.8(1)	113.8(2)	114.2(1)	114.40(9)
O_A-T-O_D	105.8(1)	106.0(1)	106.3(1)	106.3(1)	106.16(8)	106.2(1)	106.5(2)	106.6(1)	106.68(9)
O_B-T-O_C	111.1(1)	111.1(1)	111.1(1)	110.9(1)	110.67(8)	110.1(1)	110.3(2)	109.6(1)	108.97(9)
O_B-T-O_D	111.4(1)	111.4(1)	111.3(1)	111.2(1)	111.27(8)	111.6(1)	111.2(2)	111.5(1)	111.41(9)
O_C-T-O_D	108.8(1)	108.7(1)	108.5(1)	108.6(1)	108.68(7)	108.3(1)	108.1(2)	107.7(1)	107.76(9)
Mean	109.4	109.5	109.5	109.5	109.46	109.5	109.5	109.5	109.48
in $T_2(0)$									
O_A-T-O_B	109.6(1)	109.3(1)	109.3(1)	109.4(1)	109.85(8)	110.5(1)	111.2(2)	111.3(1)	112.16(9)
O_A-T-O_C	104.7(1)	104.6(1)	104.6(1)	104.6(1)	104.51(8)	104.3(1)	104.3(2)	104.2(1)	104.00(9)
O_A-T-O_D	108.6(1)	108.5(1)	108.5(1)	108.5(1)	108.32(8)	107.8(1)	107.9(2)	107.5(1)	106.73(9)
O_B-T-O_C	110.4(1)	110.7(1)	110.8(1)	110.7(1)	110.55(8)	110.8(1)	110.2(2)	110.8(1)	110.87(9)
O_B-T-O_D	111.4(1)	111.6(1)	111.6(1)	111.6(1)	111.61(8)	112.1(1)	112.0(2)	112.1(1)	112.35(9)
O_C-T-O_D	111.7(1)	111.8(1)	111.8(1)	111.7(1)	111.73(7)	111.1(1)	111.0(2)	110.6(1)	110.35(9)
Mean	109.4	109.4	109.4	109.4	109.43	109.4	109.4	109.4	109.41(9)
in $T_2(m)$									
O_A-T-O_B	109.3(1)	109.2(1)	109.2(1)	108.8(1)	108.48(8)	107.6(1)	106.8(2)	106.9(1)	105.91(9)
O_A-T-O_C	104.6(1)	104.6(1)	104.4(1)	104.8(1)	104.84(8)	104.8(1)	104.8(2)	104.6(1)	104.72(9)
O_A-T-O_D	108.6(1)	108.6(1)	108.7(1)	108.6(1)	108.91(7)	109.2(1)	109.6(2)	109.4(1)	109.87(9)
O_B-T-O_C	110.4(1)	110.4(1)	110.4(1)	110.7(1)	110.63(8)	110.7(1)	110.8(2)	110.7(1)	110.76(9)
O_B-T-O_D	111.6(1)	111.5(1)	111.6(1)	111.5(1)	111.36(8)	111.5(1)	111.4(2)	111.3(1)	111.02(9)
O_C-T-O_D	112.0(1)	112.2(1)	112.3(1)	112.2(1)	112.34(7)	112.8(1)	113.2(2)	113.5(1)	114.05(9)
Mean	109.4	109.4	109.4	109.4	109.43	109.4	109.4	109.4	109.39
$T_1(0)$-$O_A(1)$-$T_1(m)$	144.3(1)	144.3(1)	144.4(2)	144.5(1)	144.4(1)	144.2(2)	144.4(2)	144.1(1)	144.4(1)
$T_2(0)$-$O_A(2)$-$T_2(m)$	138.8(1)	139.0(1)	138.3(2)	138.9(1)	138.6(1)	138.4(2)	138.4(2)	138.3(1)	138.1(1)
$T_1(0)$-$O_B(0)$-$T_2(0)$	152.8(1)	152.7(2)	152.5(2)	152.5(1)	152.5(1)	151.8(2)	151.6(2)	151.6(1)	151.1(1)
$T_1(m)$-$O_B(m)$-$T_2(m)$	152.8(1)	152.7(2)	153.0(2)	153.2(1)	153.3(1)	153.8(2)	154.2(2)	154.6(1)	155.3(1)
$T_1(0)$-$O_C(0)$-$T_2(m)$	131.1(1)	130.9(1)	131.0(2)	131.0(1)	131.2(1)	130.8(2)	130.9(2)	130.8(1)	130.8(1)
$T_2(0)$-$O_C(m)$-$T_1(m)$	131.1(1)	130.8(1)	131.2(2)	131.1(1)	131.0(1)	131.0(2)	131.6(2)	131.4(1)	131.3(1)
$T_1(0)$-$O_D(0)$-$T_2(m)$	141.4(1)	141.7(1)	141.5(2)	141.5(1)	141.8(1)	141.1(2)	141.0(2)	140.8(1)	140.7(1)
$T_2(0)$-$O_D(m)$-$T_1(m)$	141.7(1)	141.9(1)	142.0(2)	141.9(1)	141.9(1)	141.9(2)	142.2(2)	142.5(1)	142.3(1)
Mean	141.7	141.8	141.7	141.8	141.8	141.6	141.8	141.8	141.8

Table 6. *Distortion* (σ) *of tetrahedra* (°)

	P2B	P2A	CA1A	P17C	A1D	CA1B	P1C	RC20C	CA1E
$T_1(0)$	3.056	2.966	3.008	2.977	2.961	3.248	3.161	3.236	3.357
$T_1(m)$	3.022	3.005	2.888	2.827	2.891	2.928	2.801	2.918	2.910
$T_2(0)$	2.574	2.690	2.700	2.672	2.713	2.896	2.880	3.000	3.338
$T_2(m)$	2.695	2.721	2.821	2.688	2.689	2.902	3.110	3.208	3.502

angles is generally very small, but is perhaps significant for $T_1(0)$—$O_B(0)$—$T_2(0)$ (variation 1·7°) and $T_1(m)$—$O_B(m)$—$T_2(m)$ (variation 2·6°), providing support for the suggestion that the (Al,Si) ordering process is important in determining the shape of the framework of the structure. Similar effects are discussed above in relation to K—O bond lengths (Table 4 and Fig. 2).

The anisotropic thermal displacement of the K atom in all the structures investigated is a disc-shaped ellipsoid with its minor axis almost parallel to a^*, as in the K feldspars studied previously. All the other atoms generally show only moderate anisotropy; in particular, the tetrahedral atoms do not show significant anisotropy as they do for Spencer U microcline (Bailey, 1969).

4. Atomic scattering factors and tetrahedral site occupancies

The final stages in the refinements of the structures are necessarily very complex. Thus a fractional (Al,Si) occupancy of a tetrahedral site must represent an average over the set of all the sites of that type [say, $T_1(m)$] which are in fact either AlO_4 or SiO_4. Then the temperature factor for that (Al,Si) occupancy, chosen as part of the anisotropic refinement process, must be regarded as representing both the actual thermal movements of the atoms and any variations in atomic positions, as between an AlO_4 group and an SiO_4 group, over that set of sites [$T_1(m)$].

Various procedures have been developed for handling this combination of variables: in the present study the function of Ribbe & Gibbs (1969) [hereafter RG

(1969)] and that of Smith (1974) [hereafter S (1974)] were used, and in addition unsuccessful attempts were made to refine the (Al,Si) occupancies using the program *RFINE* (Finger, 1969). For both RG (1969) and S (1974) functions equivalent isotropic temperature factors are quoted in Table 7, representing the situation at the end of the anisotropic refinement, for comparison with the isotropic temperature factor at the end of the isotropic refinement.

Table 7. *Isotropic and equivalent isotropic temperature factors using RG* (1969) *and S* (1974) *functions for the estimation of the* Al/Si *tetrahedral occupancies*

	P2B			P2A			CA1A		
	Bis.	Beq.1	Beq.2	Bis.	Beq.1	Beq.2	Bis.	Beq.1	Beq.2
K/Na	2.00	2.01	2.00	1.99	2.03	2.03	2.17	2.20	2.24
T_1(0)	0.86	0.84	0.84	0.87	0.85	0.84	0.93	0.95	0.98
T_1(m)	0.87	0.85	0.84	0.86	0.84	0.84	0.92	0.93	0.96
T_2(0)	0.75	0.79	0.80	0.74	0.80	0.80	0.86	0.87	0.93
T_2(m)	0.75	0.79	0.80	0.73	0.76	0.77	0.88	0.88	0.93
O_A(1)	1.62	1.62	1.62	1.58	1.60	1.61	1.76	1.78	1.74
O_A(2)	1.57	1.58	1.58	1.54	1.60	1.60	1.58	1.66	1.64
O_B(0)	1.89	1.83	1.83	1.85	1.85	1.84	2.09	2.07	2.03
O_B(m)	1.92	1.88	1.88	1.93	1.90	1.90	2.19	2.13	2.08
O_C(0)	1.44	1.45	1.45	1.35	1.36	1.38	1.58	1.61	1.58
O_C(m)	1.54	1.55	1.55	1.44	1.47	1.45	1.58	1.62	1.60
O_D(0)	1.51	1.52	1.52	1.42	1.48	1.49	1.56	1.63	1.60
O_D(m)	1.54	1.57	1.57	1.48	1.53	1.54	1.66	1.71	1.68
R	5.0	3.4	3.4	5.0	3.4	3.4	5.4	3.8	3.6

	P17C			A1D			CA1B		
	Bis.	Beq.1	Beq.2	Bis.	Beq.1	Beq.2	Bis.	Beq.1	Beq.2
K/Na	2.12	2.19	2.22	1.68	2.05	2.08	2.13	2.15	2.20
T_1(0)	1.03	1.04	1.06	0.64	0.78	0.82	0.89	0.90	0.92
T_1(m)	1.01	1.04	1.07	0.62	0.79	0.84	0.85	0.87	0.91
T_2(0)	0.97	0.99	1.04	0.60	0.76	0.82	0.84	0.84	0.90
T_2(m)	0.99	0.99	1.04	0.60	0.74	0.81	0.81	0.82	0.88
O_A(1)	1.90	1.94	1.89	1.16	1.60	1.59	1.65	1.68	1.65
O_A(2)	1.67	1.75	1.74	1.08	1.51	1.52	1.51	1.59	1.58
O_B(0)	2.16	2.14	2.10	1.31	1.88	1.86	1.92	1.91	1.91
O_B(m)	2.15	2.19	2.12	1.35	1.91	1.89	1.93	1.93	1.89
O_C(0)	1.66	1.71	1.68	1.08	1.46	1.47	1.45	1.51	1.51
O_C(m)	1.70	1.70	1.68	1.10	1.46	1.47	1.51	1.52	1.52
O_D(0)	1.69	1.74	1.72	1.07	1.49	1.48	1.58	1.59	1.57
O_D(m)	1.72	1.79	1.77	1.04	1.48	1.48	1.39	1.44	1.45
R	5.7	3.4	3.2	6.6	2.5	2.4	5.4	3.9	3.8

	P1C			RC20C			CA1E		
	Bis.	Beq.1	Beq.2	Bis.	Beq.1	Beq.2	Bis.	Beq.1	Beq.2
K/Na	2.08	2.12	2.16	1.81	1.88	1.91	1.55	1.65	1.69
T_1(0)	0.94	0.97	0.97	0.94	0.94	0.95	0.61	0.66	0.66
T_1(m)	0.93	0.95	1.00	0.92	0.93	0.97	0.56	0.60	0.65
T_2(0)	0.87	0.88	0.95	0.86	0.86	0.92	0.51	0.56	0.62
T_2(m)	0.88	0.88	0.94	0.88	0.88	0.94	0.53	0.57	0.63
O_A(1)	1.61	1.64	1.60	1.52	1.60	1.58	0.91	1.10	1.11
O_A(2)	1.44	1.52	1.48	1.26	1.40	1.40	0.79	0.99	1.01
O_B(0)	1.95	1.95	1.89	1.81	1.82	1.79	1.18	1.34	1.34
O_B(m)	1.86	1.92	1.89	1.91	1.97	1.94	1.36	1.54	1.52
O_C(0)	1.45	1.51	1.48	1.43	1.54	1.53	1.04	1.16	1.16
O_C(m)	1.54	1.57	1.54	1.50	1.52	1.51	1.02	1.12	1.13
O_D(0)	1.63	1.65	1.60	1.55	1.59	1.57	1.23	1.29	1.28
O_D(m)	1.61	1.66	1.62	1.45	1.56	1.54	1.11	1.25	1.25
R	6.5	5.2	5.3	5.6	3.7	3.5	4.6	3.0	2.8

Bis.:isotropic temperature factors at the end of the isotropic refinement.

Beq.1:equivalent isotropic temperature factors after Hamilton(1959) at the end of the anisotropic refinement using the Ribbe and Gibbs(1969) function.

Beq.2:equivalent isotropic temperature factors after Hamilton(1959) at the end of the anisotropic refinement using the Smith(1974) function.

It is clear that the *R* value is considerably improved for each structure when anisotropic refinement is carried out, and that the S (1974) function gives slightly better *R* values than RG (1969): these are, therefore, the values quoted as '*R* final' at the bottom of Table 1. It is interesting to note that for both functions RG (1969) and S (1974), the equivalent isotropic temperature factors (B_{eq}) are slightly larger for the T_1 pairs than for the T_2 pairs, as has been found in all previous refinements of Na and K feldspar structures. Since this difference becomes significantly smaller when the S (1974) function is used (Table 7), its physical reality may be open to question.

5. Structural symmetry of crystals P2B, P2A and CA1A

The values of α^* and γ^* (Table 1) are 90° for these three crystals, within the experimental error which is estimated as $\sim 2'$, so that the crystals are geometrically monoclinic. If they were structurally monoclinic, then pairs of reflections hkl and $h\bar{k}l$ would have identical intensities apart from small absorption errors; in fact, systematic comparison of such pairs reveals significant differences for the CA1A crystal (Table 8) and the

Table 8. *Numbers of reflection pairs in F_o ranges for different ranges of $\Delta F_o/S$*

P2B

ΔFo/S between	0-1	1-2	2-3	3-4	4-5	5-6	>6	Total pairs
20>Fo>0	212	138	59	13	12	2	4	440
40>Fo>20	140	87	48	18	2	0	1	296
60>Fo>40	49	31	23	6	2	1	0	112
80>Fo>60	11	8	2	2	2	0	0	25
Fo>80	9	10	2	0	0	0	0	21
Total pairs	421	274	134	39	18	3	5	894

P2A

ΔFo/S between	0-1	1-2	2-3	3-4	4-5	5-6	>6	Total pairs
20>Fo>0	208	145	75	26	10	11	8	483
40>Fo>20	127	73	37	27	11	2	0	277
60>Fo>40	25	36	24	9	2	6	0	102
80>Fo>60	10	8	2	1	2	0	0	23
Fo>80	6	3	5	0	2	0	0	16
Total pairs	376	265	143	63	27	19	8	901

CA1A

ΔFo/S between	0-1	1-2	2-3	3-4	4-5	5-6	>6	Total pairs
20>Fo>0	115	89	43	18	7	6	5	283
40>Fo>20	86	60	60	23	21	6	4	260
60>Fo>40	47	33	43	17	15	5	3	163
80>Fo>60	17	19	14	12	5	4	5	76
Fo>80	22	16	13	7	11	7	9	85
Total pairs	287	217	173	77	59	28	26	867

$$S=\sqrt{\frac{Fo_1^2\sigma_1^2 + Fo_2^2\sigma_2^2}{Fo_1^2+Fo_2^2}}$$

where $Fo_1 = Fo_{hkl}$ and $Fo_2 = Fo_{h\bar{k}l}$ and $\sigma_1 = \sigma Fo_{hkl}$ and $\sigma_2 = \sigma Fo_{h\bar{k}l}$

structural refinement was therefore carried out in terms of the space group $C\bar{1}$ as for the geometrically triclinic crystals. The same systematic comparison of such pairs of reflections for the P2A and P2B crystals does not permit a definite choice between monoclinic and triclinic symmetry.

The results of the structural refinement of the CA1A crystal confirm the structural triclinicity. The atomic coordinates thus determined differ significantly from values conforming to monoclinic symmetry; also the K—O distances show significant differences between pairs related by a mirror plane in monoclinic symmetry. Furthermore, the Al content estimated from T—O distances (Table 9) is significantly greater in $T_1(0)$ than in $T_1(m)$, while it is identical in $T_2(0)$ and $T_2(m)$.

In view of the ambiguity about the true symmetry of P2A and P2B, both have been refined in space group $C\bar{1}$ in order to give freedom to the refinement to tend towards the actual symmetry given by the reflection intensities. The experimental data for these two samples were collected using a halved ω-scan velocity, with 10 s background counts, in order to obtain more reliable results. The final R factor is 3·4% for both structures.

The refinement of these structures leads to the following interesting conclusions. Sample P2A is slightly but significantly triclinic: in fact $T_1(0)$ appears to be significantly larger than $T_1(m)$, the atomic coordinates generally differ by more than the standard deviations from values conforming to monoclinic symmetry (even though the differences are much smaller than for CA1A), and K—O distances also show slight triclinicity. Sample P2B, on the other hand, can be considered truly monoclinic: the dimensions of $T_1(0)$ and $T_1(m)$ do not differ significantly, nor do those of $T_2(0)$ and $T_2(m)$. The atomic coordinates show differences comparable to standard deviations from values related by a mirror plane, as do the K—O distances. Nevertheless, as in the other structures studied here, $T_1(0)$ appears slightly larger than $T_1(m)$, and K, $O_A(1)$ and $O_A(2)$ atoms move from the ideal positions of a monoclinic structure in the same directions in which, more obviously, these atoms move in the other structures. For this reason the result of the $C\bar{1}$ refinement of the structure of sample P2B has been described in terms of $C\bar{1}$ symmetry, even though it can be considered as almost perfectly 'monoclinic'.

6. The nature of the ordering process

A full discussion of the ordering process in K feldspars has been given by Smith (1974). It is generally accepted that the transition from a random distribution of Al atoms, with 0·25 Al in each $T_1(0)$, $T_1(m)$, $T_2(0)$ and $T_2(m)$ site, to perfect order, with 1·0 Al in $T_1(0)$ and little or no Al in sites $T_1(m)$, $T_2(0)$ and $T_2(m)$, may proceed by a one-step path or by a two-step path or by one of the multiple paths between. Ideally, in the first, when ordering begins Al atoms move directly from $T_1(m)$, $T_2(0)$, $T_2(m)$ into $T_1(0)$; in the two-step path, Al atoms first move from $T_2(0)$ and $T_2(m)$ into $T_1(0)$ and $T_1(m)$ and monoclinic symmetry is preserved, and in the second step Al atoms move from $T_1(m)$ into $T_1(0)$ and the symmetry is triclinic. The results obtained in the present work supplement the rather scanty experimental evidence hitherto available, and it now seems

Table 9. Al *distribution and Thompson coefficients in* K *feldspars*

	Al-contents				Total	Thompson coefficients		
Feldspar	$T_1(0)$	$T_1(m)$	$T_2(0)$	$T_2(m)$	Al	X	Y	Z
P2B	.370	.350	.150	.140	1.010	.01	.02	.43
P2A	.415	.335	.110	.110	.970	.00	.08	.53
CA1A	.470	.365	.085	.085	1.005	.00	.105	.665
P17C	.445	.330	.085	.080	.940	.005	.115	.61
A1D	.485	.305	.090	.070	.950	.02	.18	.63
CA1B	.630	.240	.065	.055	.990	.01	.39	.75
P1C	.680	.150	.065	.055	.950	.01	.53	.71
RC20C	.800	.140	.025	.025	.990	.00	.66	.89
CA1E	.900	.050	.030	.030	1.010	.00	.85	.89
High sanidine(1)	.26		.22		.96	.00	.00	.08
Heated sanidine(2)	.26		.225		.97	.00	.00	.07
Natural sanidine(3)	.32		.18		1.00	.00	.00	.28
Low sanidine(4)	.295		.195		.98	.00	.00	.20
Low sanidine(5)	.345		.125		.94	.00	.00	.44
Adularia(6)	.405		.08		.97	.00	.00	.65
Adularia(7)	.395		.07		.93	.00	.00	.65
Ordered orthoclase(8)	.43		.03		.92	.00	.00	.80
Intermediate microcline(9)	.63	.235	.045	.03	.94	.015	.395	.79
Maximum microcline(10)	.97	.015	-.01	.00	.975	-.01	.955	.975
Maximum microcline(11)	.93	.01	.055	-.025	.97	.08	.92	.91

(1) Ribbe (1963); (2) Weitz (1972); (3) Weitz (1972); (4) Phillips and Ribbe (1973); (5) Colville and Ribbe (1968); (6) Colville and Ribbe (1968); (7) Phillips and Ribbe (1973); (8) Prince, Donnay and Martin (1973); (9) Bailey (1969); (10) Brown and Bailey (1964); (11) Finney and Bailey (1964).

clear that the ordering path approximates fairly closely to the ideal two step model.

In Table 9 the Al content estimated from T—O distances for each of the four tetrahedral sites is shown on the left, in the upper part for the Adamello crystals and in the lower part for cases taken from the literature. In Fig. 3 the four tetrahedral sites for each crystal are plotted as points, each with its Al occupancy as abscissa and the Al occupancy of $T_1(0)$ as ordinate. As the Al occupancy of $T_1(0)$ increases from 0·25 (disorder), that for $T_1(m)$ increases similarly in accordance with the monoclinic symmetry while those for $T_2(0)$ and $T_2(m)$ diminish correspondingly. For crystal P2B for the first time $T_1(0)$ and $T_1(m)$ are seen to be separated as the Al occupancy of $T_1(0)$ increases at the expense of $T_1(m)$; the Al occupancies of $T_2(0)$ and $T_2(m)$, already quite small, continue to diminish slowly in successive Adamello specimens while the difference in Al occupancy for $T_1(0)$ and $T_1(m)$ continues to grow. This behaviour, characteristic of the two-step type of ordering path, is also seen in the intermediate microcline Spencer U (almost identical with CA1B) and the maximum microclines Pontiskalk and Pellotsalo (all listed in Table 9).

In Fig. 3 a 'best line' is drawn through the rather widely spread points for $T_1(m)$; in principle, its point of intersection with the $T_1(0)$ line, at Al occupancies 0·38 for $T_1(0)$ and $T_1(m)$, and therefore 0·12 for $T_2(0)$ and $T_2(m)$, fixes the boundary between monoclinic and triclinic symmetries. Too great a precision must not be claimed (in view of the 'spread' of the experimental points), but it is quite clear that the changeover is *not* located near the occupancies 0·50, 0·50, 0, 0. It is, however, interesting to note that the changeover occupancies are effectively identical with those suggested by Ferguson, Traill & Taylor (1958) (0·36, 0·36, 0·14, 0·14) as corresponding in terms of charge balance to the most stable low-temperature structure for K feldspar, which they tentatively identified as a truly monoclinic 'orthoclase'.

Not all the materials listed (from the literature) in the lower part of Table 9 conform to the two-step model described above. Adularias Spencer B (6) and 7007 (7) both have $T_1(0)$ values just below that of P2A (0·415) but just above the intersection point (0·38): neither shows $T_1(0) - T_1(m)$ separation, which would in any case be very small, and both show a domain texture. The 'ordered orthoclase' (Himalaya) (8) of Prince, Donnay & Martin (1973) also shows a domain structure. A full discussion is given by Smith (1974), but it is worthwhile to point out that the Thompson ordering coefficients listed on the right in Table 9 also lend support to the exclusion of the two adularias and the ordered orthoclase from the discussion of the ordering path. Thus in Fig. 4 the *Y* and *Z* values are plotted for all the Adamello crystals, together with those for all the other K feldspars previously studied and listed in Table 9, and it can be seen that the points for all except the adularias and ordered orthoclase lie near a smooth curve running between the ideal one-step path and the ideal two-step path, until near the value $Z = 0{\cdot}4$, $Y = 0$ where this curve intersects the ideal two-step path.

A general conclusion may be drawn about the significance of the ordering observed in the present studies of Adamello materials and earlier studies of intermediate and maximum microclines listed at the end of Table 9.

Firstly, the Adamello crystals are untwinned and precession X-ray photographs of long exposure show neither diffuse streaks near the strong reflections such as would reveal the presence of out-of-step domains, nor diffuse reflections $h + k = 2n + 1$ which would indicate loss of *C* face-centring and formation of domains with symmetry $P2_1/a$. Most of the K feldspars of the rocks from which the samples used in the present work were extracted show similar characteristics (De Pieri & Callegari, 1977).

Secondly, according to geometrical theories of twinning (Friedel, 1906; Buerger, 1945; Laves, 1950,

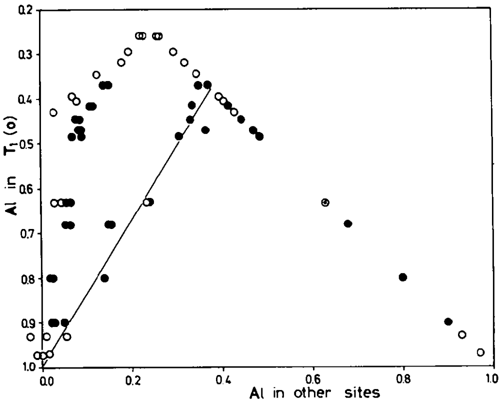

Fig. 3. Plot of Al contents for K feldspars estimated from the T—O distances listed in Table 9. Open circles refer to the literature data, solid circles to the Adamello K feldspars.

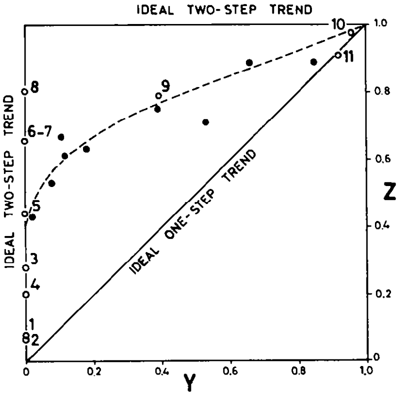

Fig. 4. Plot of Thompson ordering coefficients *Y* and *Z* for the K feldspars listed in Table 9. Solid circles refer to the Adamello K feldspars.

1952; Cahn, 1954) twinning due to phase inversion in feldspars occurs the more easily the smaller the degree of triclinicity. It is therefore concluded that the K feldspars studied in the present work have crystallized (or recrystallized) directly with triclinic symmetry and have not inverted from a primary monoclinic disordered phase through ordering due to a diffusive process. It follows that the various degrees of order of the Adamello crystals studied here, and presumably of the Spencer U, Pontiskalk and Pellotsalo microclines studied previously, represent the order corresponding to the equilibrium conditions at the moment of crystallization or of a possible subsequent recrystallization.

This work was carried out through the financial support of the Consiglio Nazionale delle Ricerche (CT 77.01139.05, Padova, and the Centro di Studio per la Cristallografia Strutturale, Università di Pavia).

References

BAILEY, S. W. (1969). *Am. Mineral.* **54**, 1540–1545.
BROWN, B. E. & BAILEY, S. W. (1964). *Acta Cryst.* **17**, 1391–1400.
BUERGER, M. J. (1945). *Am. Mineral.* **30**, 469–482.
BUSING, W. R., MARTIN, K. O. & LEVY, H. A. (1962). *ORFLS*. Report ORNL-TM-305. Oak Ridge National Laboratory, Tennessee.
CAHN, R. W. (1954). *Adv. Phys.* **3**, 363–445.
CALLEGARI, E., DE PIERI, R., MEZZACASA, G. & PICCIRILLO, E. M. (1974). *Mem. Ist. Geol. Mineral. Univ. Padova*, **31**, 1–35.
COLVILLE, A. A. & RIBBE, P. H. (1968). *Am. Mineral.* **53**, 25–37.
DAVIES, J. E. & GATEHOUSE, B. M. (1973). *Acta Cryst.* B**29**, 1934–1942.
DE PIERI, R. & CALLEGARI, E. (1977). *Mem. Sci. Geol.* **32**, 1–16.
FERGUSON, R. B., TRAILL, R. J. & TAYLOR, W. H. (1958). *Acta Cryst.* **11**, 331–348.
FINGER, L. W. (1969). *Carnegie Inst. Washington Yearb.* **67**, 216–217.
FINNEY, J. J. & BAILEY, S. W. (1964). *Z. Kristallogr.* **119**, 413–436.
FRIEDEL, G. (1906). *Leçons de Cristallographie.* Paris: Hermann.
GOLDSMITH, J. R. & LAVES, F. (1954). *Geochim. Cosmochim. Acta*, **6**, 100–118.
HAMILTON, W. C. (1959). *Acta Cryst.* **12**, 609–610.
International Tables for X-ray Crystallography (1962). Vol. III. Birmingham: Kynoch Press.
LAVES, F. (1950). *J. Geol.* **58**, 548–571.
LAVES, F. (1952). *Naturwissenschaften*, **39**, 546–547.
PHILLIPS, M. W. & RIBBE, P. H. (1973). *Am. Mineral.* **58**, 263–270.
PRINCE, E., DONNAY, G. & MARTIN, R. F. (1973). *Am. Mineral.* **58**, 500–507.
RIBBE, P. H. (1963). *Acta Cryst.* **16**, 426–427.
RIBBE, P. H. & GIBBS, G. V. (1969). *Am. Mineral.* **54**, 85–94.
RIBBE, P. H., PHILLIPS, M. W. & GIBBS, G. V. (1972). Program for Advanced Study Institute on Feldspars, July, Manchester.
SMITH, J. V. (1974). *Feldspar Minerals.* New York: Springer.
WEITZ, G. (1972). *Z. Kristallogr.* **136**, 418–426.

Acta Cryst. (1978). B**34**, 2707–2711

The Crystal Structure of Strontium Uranyl Tetraformate Hydrate: $SrUO_2(HCOO)_4.(1 + x)H_2O$

BY BERNARD F. MENTZEN, JEAN-PIERRE PUAUX AND HENRY SAUTEREAU

Laboratoire de Cinétique et Génie Chimiques, INSA de Lyon, 20 *avenue Albert Einstein, F*-69621, *Villeurbanne, France*

(*Received* 25 *January* 1978; *accepted* 16 *March* 1978)

The crystal structure of strontium uranyl tetraformate hydrate has been established by X-ray diffraction at room temperature. This compound crystallizes in the orthorhombic space group *Pbca* with $a = 6{\cdot}449$ (1), $b = 16{\cdot}393$ (3) and $c = 20{\cdot}740$ (3) Å; $Z = 8$. The structure has been determined by the heavy-atom method from 2352 Mo $K\bar{\alpha}$ intensities measured on a four-circle automatic diffractometer and refined by full-matrix least-squares computations. The final weighted residual is 0·0468 (conventional $R = 0{\cdot}0463$). The U atom is surrounded by a pentagonal bipyramid of O atoms. The apical O atoms are those of the uranyl group, which is not quite linear [O—U—O = 175·5 (2)°]. The formato groups all bridge either two U atoms or U and Sr atoms. The O atom of the water molecule (O*W*) belongs to the coordination polyhedron of the Sr atom [Sr—O*W* = 2·509 (5) Å], which is a capped octahedron (seven-coordinate polyhedron) of O atoms. The structure reveals the presence of two kinds of channels running parallel to the [100] direction; one of them allows the presence of interstitial water (xH_2O) as shown by chemical analysis.